BIOCHEMISTRY
including biophysical chemistry & molecular biology

Article

pubs.acs.org/biochemistry

The G-Quadruplex Augments Translation in the 5′ Untranslated Region of Transforming Growth Factor β2

Prachi Agarwala,[†] Satyaprakash Pandey,[†] Koyeli Mapa,[†] and Souvik Maiti*[,†,‡]

[†]Proteomics and Structural Biology Unit, Institute of Genomics and Integrative Biology, CSIR, Mall Road, Delhi 110007, India
[‡]National Chemical Laboratory, CSIR, Dr. Homi Bhabha Road, Pune 411008, India

Supporting Information

ABSTRACT: Transforming growth factor β2 (TGFβ2) is a versatile cytokine with a prominent role in cell migration, invasion, cellular development, and immunomodulation. TGFβ2 promotes the malignancy of tumors by inducing epithelial−mesenchymal transition, angiogenesis, and immunosuppression. As it is well-documented that nucleic acid secondary structure can regulate gene expression, we assessed whether any secondary motif regulates its expression at the post-transcriptional level. Bioinformatics analysis predicts an existence of a 23-nucleotide putative G-quadruplex sequence (PG4) in the 5′ untranslated region (UTR) of TGFβ2 mRNA. The ability of this stretch of sequence to form a highly stable, intramolecular parallel quadruplex was demonstrated using ultraviolet and circular dichroism spectroscopy. Footprinting studies further validated its existence in the presence of a neighboring nucleotide sequence. Following structural characterization, we evaluated the biological relevance of this secondary motif using a dual luciferase assay. Although PG4 inhibits the expression of the reporter gene, its presence in the context of the entire 5′ UTR sequence interestingly enhances gene expression. Mutation or removal of the G-quadruplex sequence from the 5′ UTR of the gene diminished the level of expression of this gene at the translational level. Thus, here we highlight an activating role of the G-quadruplex in modulating gene expression of TGFβ2 at the translational level and its potential to be used as a target for the development of therapeutics against cancer.

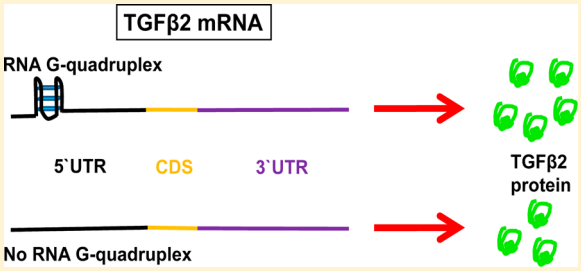

G-Quadruplexes are found in G-rich sequences of DNA and RNA.[1,2] These are noncanonical four-stranded secondary structures formed by two or more stacks of G-quartets held together by Hoogsteen base pairing.[3−5] Although a considerable amount of work has been done on the DNA G-quadruplex in past three decades, recent years saw a gradual shift toward understanding the G-quadruplexes at the RNA level. In RNA, G-quadruplexes have been associated with translational regulation,[6−17] 3′ end processing,[18,19] transcription termination,[20] alternative splicing,[21−24] mRNA localization,[25] protein binding,[26−28] and telomeric RNA biology.[29−34] The genomewide computational analysis has revealed the presence of 4141 G-quadruplex motifs in the 5′ UTR of mRNAs.[35] The functional relevance of this secondary structure has been validated experimentally in sequences in FGF-2,[6] NRAS,[7] Zic-1,[8] exon C of human and bovine estrogen receptor R,[9,10] MT3-MMP,[12] BCL2,[13] TRF-2,[15] VEGF,[14] and ADAM-10.[16] Except for VEGF, the RNA G-quadruplex in the 5′ UTR of the reported genes mentioned above is shown to repress gene expression at the translational level. Herein, we decipher the unusual activating role of the RNA G-quadruplex in the context of the entire 5′ UTR of TGFβ2 mRNA.

TGFβ2 is a pleiotropic cytokine with multiple roles in cell proliferation, differentiation, embryogenesis, migration, tissue repair, and modulation of the immune response.[35] TGFβ2 is a major cytokine found in the body fluids such as amniotic fluid, breast milk, and the aqueous and vitreous humor of the eye.[36] It is strongly expressed at an early stage of epicardial vascular formation and plays an important role in epicardial biology.[37] The TGFβ2 knockout mice show perinatal mortality and a wide range of developmental defects, including cardiac defects.[38,39] The abnormal expression of this protein is also associated with various eye-related diseases.[40] Furthermore, the tumors of numerous histogenetic origins have been reported to synthesize and release TGFβ2.[41−50] It is overexpressed especially in the later stages of carcinogenesis, causing epithelial−mesenchymal transition (EMT), tumor invasiveness, and metastasis.

With such an important role in immunomodulation and tumor progression, it is quite obvious that its expression is regulated at various levels of gene expression. A polymorphism in the promoter region of the TGFβ2 gene significantly increases its transcriptional activity in breast cancer cells.[51] miR-200a and miR-141 bind to the 3′ UTR of TGFβ2 mRNA to inhibit its translation.[52] Bioinformatics analysis showed the presence of putative G-quadruplex sequence in the 5′ UTR of TGFβ2 mRNA.[53]We evaluated the role of this secondary structure as a cis regulatory element in TGFβ2 mRNA translation.

Received: October 5, 2012
Revised: January 30, 2013
Published: February 6, 2013

dx.doi.org/10.1021/bi301365g | *Biochemistry* 2013, 52, 1528−1538

Table 1. Sequences of Oligonucleotides Used for the Biophysical Studies

oligonucleotide name	sequence (5′−3′)
PG4 RNA	GGGAAAGGGUGGGAGUCCAAGGG
mPG4 RNA	GAGAAAGAGUGAGAGUCCAAGAG
9-PG4−9 RNA	GCAGAGGUUGGGAAAGGGUGGGAGUCCAAGGGAGCCCCUGC
m9-PG4−9 RNA	GCAGAGGUUCGCAAAGGGUGGGAGUCCAAGCGAGCCCCUGC

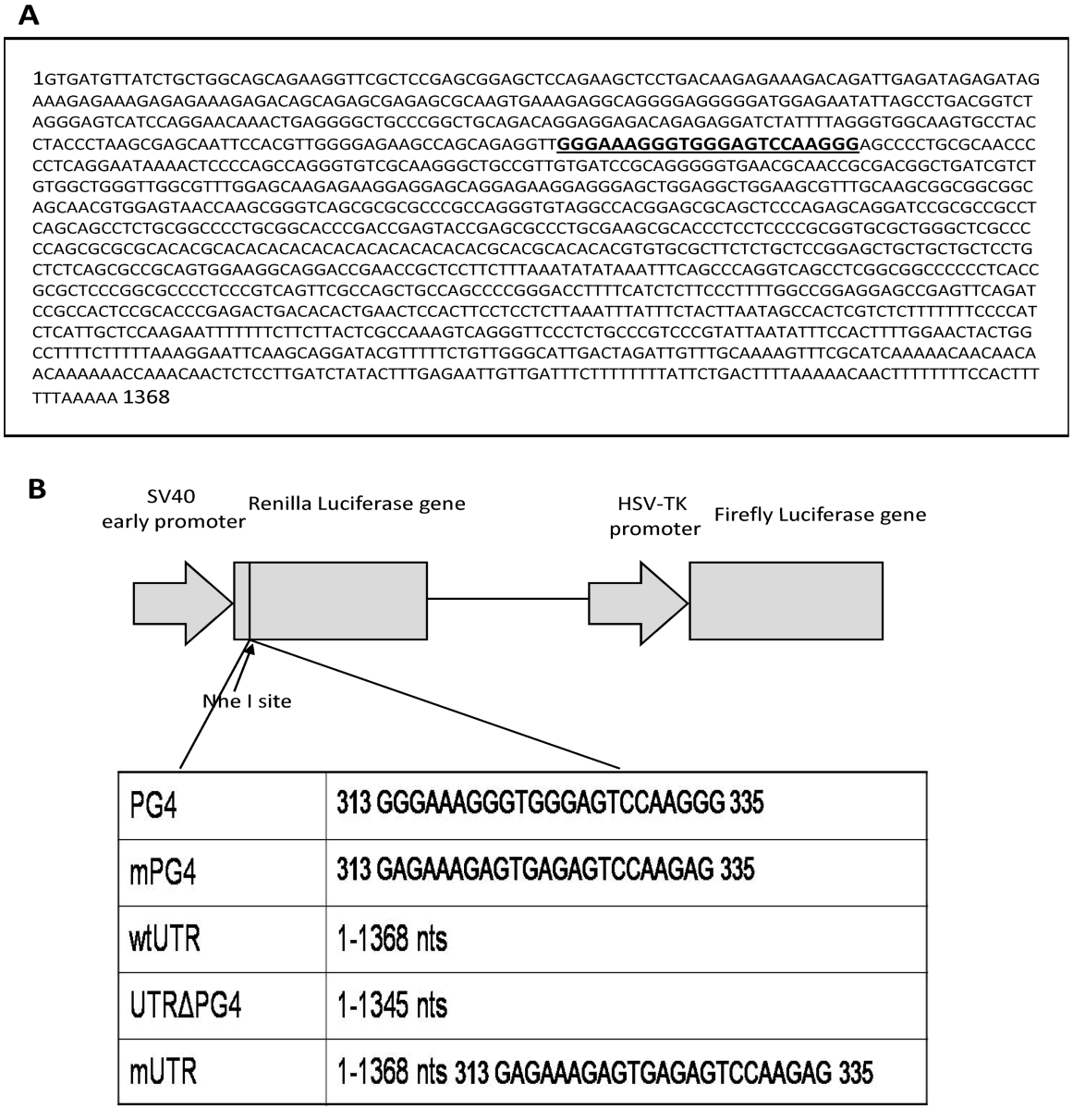

Figure 1. Schematic representation of the 5′ UTR of TGFβ2 and constructs used for transfection. (A) Representation of the entire 1368-nucleotide 5′ UTR of TGFβ2. The putative G-quadruplex-forming sequence (PG4) is underlined and shown in bold. PG4 lies between nucleotide 313 and nucleotide 335 of the 5′ UTR of TGFβ2. (B) Schematic representation of the constructs used for transfection studies. PG4, mPG4, wtUTR, UTRΔPG4, and mUTR sequences are inserted at the NheI restriction enzyme site upstream of the Renilla luciferase gene and downstream of the SV40 promoter.

In this study, we assessed the ability of the putative G-quadruplex forming sequence in the 5′ UTR of TGFβ2 (GenBank entry NM_001135599.2) to form a stable G-quadruplex using standard biophysical techniques and studied its biological relevance in human cells. We performed a series of spectroscopic studies to characterize this motif thermodynamically and luciferase reporter assays to evaluate its functional role in modulating translational efficacy. Interestingly, in contrast to the generally reported inhibitory role of the RNA G-quadruplex, we found that the RNA G-quadruplex in the 5′ UTR of TGFβ2 is involved in the upregulation of gene expression at the translational level.

MATERIALS AND METHODS

Oligonucleotides. The high-performance liquid chromatography-purified PG4 RNA and mPG4 RNA oligonucleotides were purchased from Sigma, and 9-PG4−9 RNA and m9-PG4−9 RNA oligonucleotides were purchased from IBA (Table 1). The

dx.doi.org/10.1021/bi301365g | Biochemistry 2013, 52, 1528−1538

concentration of RNA was measured with a UV spectrophotometer and calculated using their molar extinction coefficients.

The DNA oligonucleotides for cloning were purchased from Sigma (Tables S1 and S3 of the Supporting Information).

CD Spectroscopy. RNA samples were prepared at a concentration of 2 μM in 10 mM cacodylate buffer (pH 7.4) containing 25 mM KCl salt. The samples were heated at 95 °C for 5 min and slowly cooled to 4 °C. CD experiments were performed in a Jasco J-810 spectropolarimeter (Jasco Hachioji, Tokyo, Japan) equipped with a Peltier temperature controller, and scans were taken at wavelengths of 200−350 nm at 20 °C. Following the subtraction of the buffer alone, the CD scans were taken in triplicate, and the average was calculated. CD melting of RNA oligonucleotides was performed at a rate of 0.2 °C/min from 15 to 95 °C, and readings were collected every 5 °C. The melting curves were analyzed using Origin version 7.0. CD melting data were further analyzed for calculating thermodynamic parameters (within 10% error) using Mathematica version 5.0. The ellipticity values obtained at 263 nm were evaluated by a nonlinear least-squares curve fitting method. This method involved the contribution from pre- and post-transition baselines, and thermodynamic data were obtained using equations described previously.[54]

$$A_u = b_u + (m_u T) \quad (1)$$

$$A_l = b_l + (m_l T) \quad (2)$$

$$K_{eq} = (1 - \alpha)/\alpha \quad (3)$$

$$\theta(T) = \alpha(\theta_u - \theta_l) + \theta_l \quad (4)$$

$$K_{eq} = \exp\left(\frac{\Delta G^\circ}{RT}\right) = \exp\left(\frac{\Delta H^\circ}{RT} + \frac{\Delta S^\circ}{RT}\right) \quad (5)$$

where A_u and A_l are linear equations for the upper and lower baselines, respectively, b_u and b_l describe fitted parameters for the intercepts for the upper and lower baseline with m_u and m_l as their slopes, respectively, K_{eq} indicates the equilibrium constant for the unstructured−structured transition for an intramolecular system, and α stands for the folded fraction. $\theta(T)$, the dependent variable, is the experimentally determined ellipticity at each temperature (T). These equations were used to calculate the van't Hoff enthalpy (ΔH_{vH}) and entropy (ΔS_{vH}).

UV Spectroscopy. UV melting studies were conducted using a Cary 100 UV−visible spectrophotometer (Varian) equipped with a Peltier temperature controller. Samples were heated to 95 °C and slowly cooled to 15 °C at a rate of 0.2 °C/min. The absorption data were collected at 298 nm at 0.2 min data intervals of heating and melting steps. UV melting of 2−20 μM samples was also performed.

Thermal Difference Spectrum (TDS). RNA oligonucleotides at the concentration of 2 μM were UV scanned over the wavelength range of 200−350 nm at 20 and 95 °C using a Cary 100 UV−visible spectrophotometer (Varian). The UV absorbance data obtained at these two temperatures were subtracted from each other and plotted on a graph to obtain TDS.

Radiolabeling of RNA. RNA oligonucleotides (with nine-nucleotide flanks) were purchased from IBA. Oligonucleotides were radiolabeled using the Kinase Max kit (Ambion) as per the protocol provided by the manufacturer. Briefly, the RNA was incubated with T4 polynucleotide kinase and [γ-^{32}P]ATP for 1 h at 37 °C. We stopped the reaction using 1 mM EDTA and by heating the mixture at 95 °C for 2 min. The labeled RNA was further purified using NucAway columns (Ambion).

RNase T1 Footprinting. The 5′ end-radiolabeled RNAs were heated at 90 °C for 5 min and then allowed to cool to 37 °C in 1 mM $MgCl_2$, 150 mM KCl, and 150 mM LiCl to facilitate structure formation. Structured RNA was digested with 0.025 unit of RNase T1 for 5 min at 37 °C. To obtain the corresponding ladder, alkaline hydrolysis of RNA was performed at 90 °C in sodium bicarbonate buffer for 10 min. RNase T1 ladder was formed by digesting the RNA in buffer containing 20 mM Tris-HCl (pH 7.5), 10 mM $MgCl_2$, and 100 mM LiCl for 2 min at 37 °C with 0.6 unit of RNase T1. We stopped all reactions by adding stop buffer containing 95% formamide and 18 mM EDTA and subsequently immediately snap chilling the mixtures on dry ice. Equal counts of digested products were separated on a 15% denaturing gel in 0.5× Tris-borate EDTA buffer and exposed to a phosphorimager screen. The gel images were scanned on a Typhoon scanner (GE Healthcare).

Plasmid Construction. The entire 5′ UTR of TGFβ2 (Figure 1) was inserted into the NheI restriction site at the 5′ region of the Renilla luciferase gene of plasmid psiCHECK-2 (Promega), and this plasmid construct was named pwtUTR. Briefly, the primers for cloning of the entire 5′ UTR of TGFβ2 were designed according to GenBank entry NM_001135599.2. Then the entire 5′ UTR of TGFβ2 was amplified via polymerase chain reaction (PCR) from genomic DNA (isolated from PBMCs) using Phusion DNA polymerase (New England Biolabs). The PCR product was gel eluted using the Qiagen gel extraction kit. The eluted PCR products and psiCHECK-2 vector were digested with the NheI restriction enzyme and again purified using the PCR purification kit (Qiagen). The digested psiCHECK-2 vector was dephosphorylated at the 5′ end using calf intestinal alkaline phosphatase (NEB) to prevent self-ligation. The digested PCR product was inserted at the NheI restriction site of the dephosphorylated vector using the T4 DNA ligase (Fermentas) enzyme at 22 °C for 16 h. The clones obtained were digested with the NheI restriction enzyme and run on agarose gel to check insert release. The positive clones obtained were then confirmed by sequencing.

Site-directed mutagenesis at specific positions of the 5′ UTR of TGFβ2 (pmUTR, pG313AUTR, and pG313A,G321AUTR) was performed using Phusion DNA polymerase. Briefly, the wtUTR construct was amplified via PCR with primers containing site-directed mutations at an annealing temperature of 55 °C using Phusion DNA polymerase. The amplified products were digested with the DpnI enzyme (NEB) at 37 °C for 6 h. The *Escherichia coli* DH5α cells were then transformed with these products. The clones obtained were checked for insert release and finally analyzed by sequencing.

The 23-nucleotide putative G-quadruplex-forming sequence was deleted from the 5′ UTR region of TGFβ2 (pUTRΔPG4) using deletion mutagenesis. Briefly, the 312 and 1034 bp upstream and downstream of the PG4 sequence, respectively, were separately amplified via PCR using Phusion DNA polymerase. The amplicons obtained were PCR overlapped to obtain the entire 5′ UTR region of TGFβ2 without the 23-nucleotide PG4 sequence. The gel-purified products were digested and ligated with the psiCHECK-2 vector using the method described above.

Both strands of PG4 and mPG4 sequences were heated at 94 °C and subsequently annealed at 37 °C for 1 h. Then the annealed products were inserted into the NheI restriction site of the dephosphorylated psiCHECK-2 vector using T4 DNA ligase.

dx.doi.org/10.1021/bi301365g | *Biochemistry* 2013, 52, 1528−1538

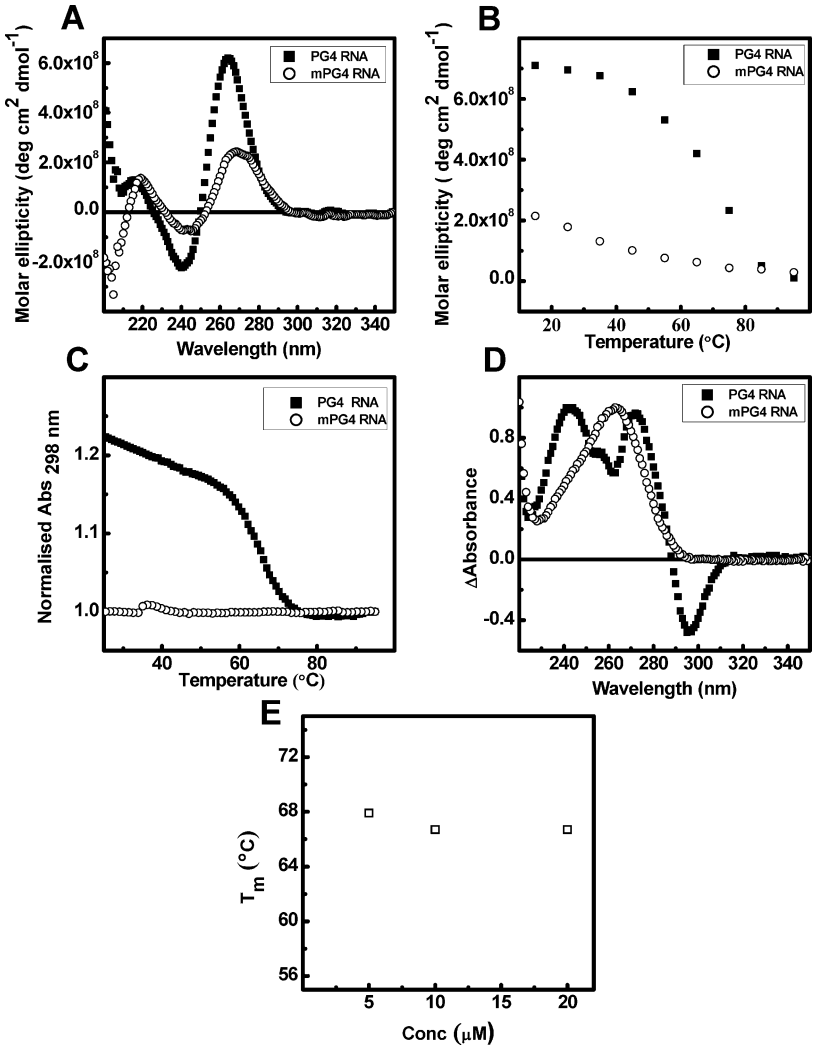

Figure 2. Biophysical characterization of PG4 RNA and mPG4 RNA. (A) Circular dichroism spectra of 2 μM PG4 RNA (■) and 2 μM mPG4 RNA (○). (B) CD melting of 2 μM PG4 RNA (■) and 2 μM mPG4 RNA (○) at 263 nm. (C) UV melting of PG4 RNA (■) and mPG4 RNA (○) at 298 nm. (D) Thermal difference spectrum of 2 μM PG4 RNA (■) and 2 μM mPG4 RNA (○). (E) T_m of PG4 RNA at different strand concentrations. T_m is found to be independent of RNA strand concentration, indicating intramolecular G-quadruplex formation. All these experiments were performed in 10 mM sodium cacodylate buffer (pH 7.4) containing 25 mM KCl.

Positive clones (pPG4 and pmPG4 plasmid constructs) were obtained by sequencing.

Cell Culture. HEK 293T and MCF-7 cell lines were maintained in a humidified atmosphere containing 5% CO_2 at 37 °C. The cells were grown in the high-glucose Dulbecco minimal Eagle's medium (DMEM) supplemented with heat-inactivated 10% fetal bovine serum and antibiotic-antimycotic (Gibco).

Dual Luciferase Assay. HEK 293T and MCF-7 cells were transfected with psiCHECK2 clones with pPG4, pmPG4, the entire 5′ UTR (pwtUTR), mutated 5′ UTR inserts (pmUTR), and the UTR with deleted PG4 inserts (pUTRΔPG4) using lipofectamine reagent (Invitrogen). The dual luciferase assay of cell lysates was performed after transfection for 48 h. The transfected cells in the 24-well plates were treated with passive lysis buffer (Promega). Renilla and firefly luciferase activity of the cell lysate was measured by using the dual luciferase reporter assay kit (Promega) and TECAN plate reader. The ratio of Renilla luciferase activity to firefly luciferase activity was calculated, and the value obtained was normalized against the empty vector/pmUTR luciferase readings.

Quantitative Real-Time PCR. HEK 293T and MCF-7 cells were transfected in six-well plates with the plasmid constructs mentioned above, and the mRNA levels of Renilla and firefly luciferase genes were quantified by real-time PCR. Briefly, the total cellular RNA of the transfected cells was isolated using the Trizol method. The quality of the RNA was assessed on the 1% agarose gel. Then the cDNA was prepared using oligo-dT and RevertAid MMLV Reverse Transcriptase enzyme (Fermentas). Following cDNA synthesis, the forward and reverse primers for Renilla and firefly luciferase genes (Table S2 of the Supporting Information) were used to amplify the transcripts of these genes by real-time PCR using a SYBR-Green PCR Master Mix (Applied Biosystems) and the Roche detection system. The Renilla/firefly transcript level ratio was calculated, normalized using the Pfaffl method,[55] and depicted in a histogram.

UV−Vis Absorption Titration. The absorption spectra were recorded on a Cary100 UV−vis double-beam spectrophotometer by stepwise addition of PG4 RNA to the 1 cm path length cuvette containing 1.44 μM TmPyP4 [5,10,15,20-tetrakis(*N*-methyl-4-pyridyl)porphyrin]. The readings were taken in the wavelength range of 350−550 nm at 25 °C. The titrations were

dx.doi.org/10.1021/bi301365g | *Biochemistry* 2013, 52, 1528−1538

terminated when the wavelength and intensity of the absorption band did not change with three successive additions of PG4 RNA.

The concentrations of the free ligand (C_f) and the bound ligand (C_b) were calculated using the equations $C_f = C(1 - \alpha)$ and $C_b = C_T - C_f$, respectively, where C_T stands for the total concentration of ligand TmPyP4. The fraction of bound ligand TMPyP4 (α) was calculated using the equation $\alpha = (A_f - A)/(A_f - A_b)$, where A_f and A_b represent the absorbance value of the free and fully bound TMPyP4, respectively, at the Soret maximum (421 nm) of TMPyP4 and A is the absorbance value at 421 nm at any given point during the titration. The percent hypochromicity of the Soret band of TMPyP4 was calculated using the equation percent hypochromicity = $[(\varepsilon_f - \varepsilon_b)/\varepsilon_f] \times 100$, where ε_b and ε_f values are calculated using the equations $\varepsilon_b = A_b/C_b$ and $\varepsilon_f = A_f/C_f$, respectively.

Treatment of Transfected Cells with Porphyrin TmPyP4. MCF-7 cells were transfected with pwtUTR, pmUTR, and pUTRΔPG4 using lipofectamine reagent (Invitrogen). After transfection for 4 h, the medium was replaced with the DMEM containing varying concentrations (5, 10, and 50 μM) of TmPyP4. After TmPyP4 treatment for 24 h, the dual luciferase assay was performed with cell lysates. The ratio of Renilla luciferase activity to firefly luciferase activity was calculated. In each case, the value obtained was normalized against luciferase readings of the transfected cells without TmPyP4 treatment.

RESULTS

The TGFβ2 gene is mapped at chromosomal location 1q41. Bioinformatics algorithm Quadfinder[53] predicts the occurrence of the putative G-quadruplex sequence (PG4) at nucleotide position 313 from the 5′ end of TGFβ2 mRNA. This PG4 sequence is located 1056 nucleotides upstream of the translation start site in the 1368-nucleotide 5′ UTR of TGFβ2 mRNA. This motif is absent in the promoter region of the TGFβ2 gene, 2 kb upstream from the transcription start site.

The PG4 Sequence Forms a Stable G-Quadruplex Motif in Vitro. Circular dichroism is a standard technique used for the structural characterization of G-quadruplex motifs. As shown in Figure 2A and Figure S5A of the Supporting Information, the CD spectrum of PG4 RNA reveals a positive peak at 264 nm and a negative peak at 240 nm. This CD spectrum corresponds to the characteristic CD signature of the parallel G-quadruplex. However, the mutated version of this oligonucleotide (mPG4 RNA) where guanosines at four positions have been replaced with adenosine shows a hypochromic shift with a molar ellipticity at 264 nm that is reduced to one-third of that of wild-type RNA. Besides, mPG4 shows a positive peak at 268 nm and a negative peak at 245 nm, indicating that the mutated PG4 sequence is unable to form stable G-quadruplex structure.

To assess the stability of the PG4 RNA G-quadruplex, CD melting was performed. CD melting (Figure 2B and Figure S1 of the Supporting Information) of PG4 RNA in 25 mM KCl showed a pronounced hypochromic shift at 263 nm when the RNA was heated from 15 to 95 °C, and a plot of CD signal at 263 nm versus temperature shows sigmoidal behavior indicating quadruplex melting. CD melting analysis revealed a T_m of 64 ± 1 °C. On the other hand, such a sigmoidal curve was absent in the case of mPG4 and hence indicates the absence of quadruplex structure in mPG4 RNA due to mutation of guanine residues. The values of thermodynamic variables are listed in Table 2. It shows that PG4 RNA G-quadruplex formation is thermodynamically favorable at 25 °C with a ΔG of −7.91 kcal/mol. Though its formation is entropically unfavorable, the high favorable enthalpy compensates by the same amount and contributes to its thermodynamic stability.

Table 2. T_m Values and Thermodynamic Parameters Calculated from the CD Melting of Various Oligonucleotides[a]

oligonucleotide	T_m[b] (°C)	ΔH (kcal/mol)	ΔS (cal mol^{-1} K^{-1})	ΔG[c] (kcal/mol)
PG4 RNA	64	−66.63	−197.06	−7.91
mPG4 RNA	ND[d]	ND[d]	ND[d]	ND[d]
9-PG4−9 RNA	69	−77.76	−227.11	−10.08
m9-PG4−9 RNA	66	−93.87	−277.27	−11.24

[a]All experiments were conducted in 10 mM sodium cacodylate buffer (pH 7.4) containing 25 mM KCl. The thermodynamic parameters reported are within 10% error. [b]The reported T_m values have an associated error of ±1 °C. [c]ΔG was calculated at 25 °C. [d]Not defined.

To validate the observations from CD studies, thermal melting was performed.[56] The UV melting profile of PG4 RNA (Figure 2C) in 10 mM sodium cacodylate (pH 7.4) containing 25 mM KCl showed the characteristic hypochromic sigmoidal transition at 298 nm. This hypochromic shift at 298 nm is the signature of the G-quadruplex secondary structure. The T_m calculated from the thermal curve is 64.8 ± 1 °C, which is similar to the value obtained via CD melting within experimental error. With increasing salt concentrations, the PG4 RNA sequence also shows a pronounced increase in T_m, which in turn indicates stabilization of the quadruplex structure (Figure S2 of the Supporting Information). To assess whether the formed quadruplex is intra- or intermolecular in nature, a melting experiment was conducted at different oligonucleotide concentrations. Further, a concentration-dependent study of PG4 RNA revealed the intramolecular status of its G-quadruplex. As shown in Figure 2E, the T_m of a different strand concentration of PG4 RNA is found to be approximately similar, demonstrating formation of the intramolecular G-quadruplex.

Furthermore, the thermal difference spectrum (TDS) of PG4 RNA and mPG4 RNA was drawn and analyzed. The TDS is the spectrum obtained by subtracting the values of the ultraviolet absorbance of the nucleic acids in the folded and unfolded state at the temperatures above and below the T_m and over the wavelength range.[57] The PG4 RNA TDS, calculated from UV absorbance data recorded at 20 and 95 °C, gave two characteristic positive peaks at 241 and 272 nm and a negative peak at 298 nm. This characteristic signature of the G-quadruplex at 298 nm was absent from the mutated version of this oligonucleotide. The mPG4 RNA gave only one positive peak at 263 nm and no negative peaks (Figure 2D).

The PG4 Sequence with Flanks Also Shows Stable G-Quadruplex Motif Signals. In the DNA quadruplex, flanking bases influence the formation and stability of G-quadruplexes. Arora et al. have shown that in the c-kit gene when the flank length exceeds eight nucleotides, the propensity to form DNA G-quadruplex decreases.[58] Thus, to access the influence of flanking nucleotide sequence on G-quadruplex formation at the RNA level, we took a PG4 sequence with nine-nucleotide flanks on each side (9-PG4−9 RNA) and characterized it biophysically.

To determine the secondary structure of 9-PG4−9 RNA, CD spectroscopy was performed. As shown in Figure 3A and Figure S5B of the Supporting Information, the CD spectrum of 9-PG4−9 RNA reveals a positive peak at 264 nm and a negative peak at

dx.doi.org/10.1021/bi301365g | Biochemistry 2013, 52, 1528−1538

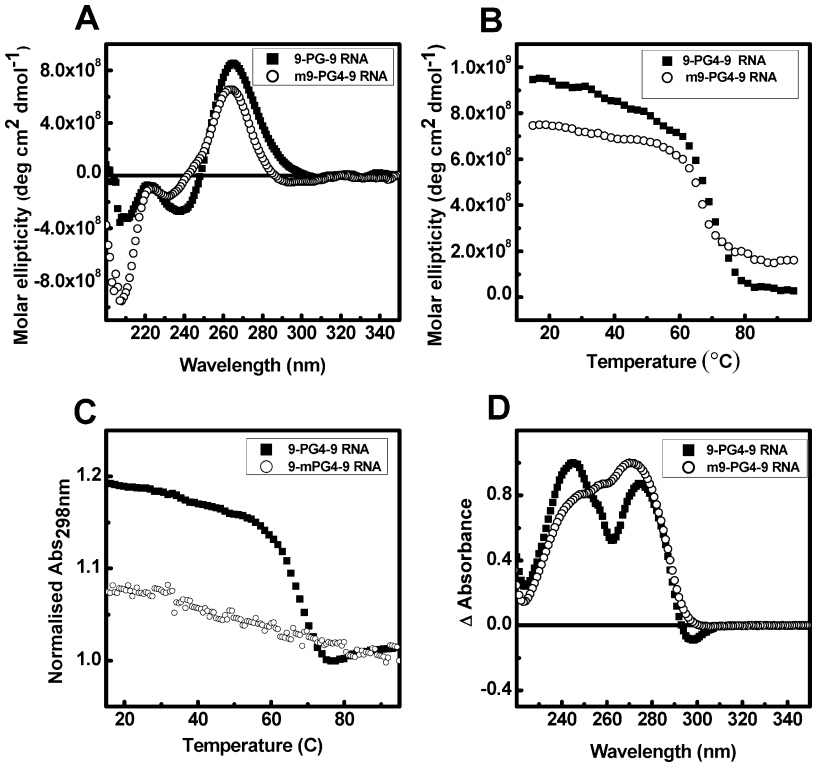

Figure 3. Biophysical characterization of 9-PG4−9 and m9-PG4−9 RNA. (A) CD spectra of 2 μM 9-PG4−9 RNA (■) and 2 μM m9-PG4−9 RNA (○). (B) CD melting of 2 μM 9-PG4−9 RNA (■) and 2 μM m9-PG4−9 RNA (○) at 263 nm. (C) UV melting of 2 μM 9-PG4−9RNA (■) and 2 μM m9-PG4−9 RNA (○) at 298 nm. (D) Thermal difference spectrum of 2 μM 9-PG4−9 RNA (■) and 2 μM m9-PG4−9 RNA (○). All these experiments were performed in 10 mM sodium cacodylate buffer (pH 7.4) containing 25 mM KCl.

240 nm. Again the mutated version of the same oligonucleotide (m9-PG4−9 RNA) showed an intense negative peak at 207 nm, a signature characteristic of RNA duplex. The CD melting profile of RNA oligonucleotides with nine-nucleotides flanks is shown in Figure 3B and Figure S1 of the Supporting Information. Upon addition of nine-nucleotide flanks on either end of PG4, an increment of 5 °C in the T_m of 9-PG4−9 RNA was observed, signifying further stabilization of the G-quadruplex structure in the presence of flanking sequence. CD melting of m9-PG4−9 RNA also showed a hypochromic shift at 263 nm. However, this shift was confronted by its UV melting at 298 nm (Figure 3C). At this wavelength, m9-PG4−9 RNA was unable to show a hypochromic shift with an increase in temperature, suggesting the absence of G-quadruplex formation. Thus, the hypochromic shift at 263 nm observed in CD melting of m9-PG4−9 RNA was a consequence of duplex melting. The UV melting of 9-PG4−9 RNA at 298 nm again demonstrated a characteristic G-quadruplex sigmoidal curve with a T_m of 68.5 ± 1 °C, which correlates well with its CD melting-derived T_m value within experimental error.

The TDS of 9-PG4−9 RNA reveals two positive peaks at 245 and 274 nm and a negative peak at 298 nm, suggesting a predisposition of the oligonucleotide to form G-quadruplex. The mutant version of 9-PG4−9 (m9-PG4−9) RNA's TDS profile shows a complete absence of these characteristic G-quadruplex peaks at 245, 274, and 298 nm (Figure 3D).

A Footprinting Assay Shows a PG4 Sequence with Flanks Favors Quadruplex Formation. To ascertain the formation of the quadruplex in the wild-type TGFβ2 quadruplex sequence, enzymatic probing was performed in the presence of potassium ions, lithium ions, and divalent magnesium ions. Potassium ions are known to stabilize G-quadruplex structures much more than lithium ions do, while quadruplex formation does not depend upon divalent magnesium ions. RNase T1 footprinting is used to determine the features of secondary structure formed in an oligonucleotide. RNase T1 cleaves after guanine residues in single-stranded ribonucleic acids. Thus, the guanines involved in secondary structure formation would be protected from RNase T1 cleavage, and this protection would be reflected in the form of less intense bands in gels in comparison to the bands resulting from structurally unstrained guanine residues.[12,14]

9-PG4−9 RNA was heated and cooled in magnesium buffer (Mg^{2+}), potassium buffer (K^+), and lithium buffer (Li^+) and subjected to enzymatic digestion. Subsequent footprinting analysis of these oligonucleotides revealed protection of 9-PG4−9 RNA from cleavage at guanine residues G10−G12, G16−G18, G20−G22, and G30−G32 (highlighted in Figure 4A). These guanine residues are predicted to be involved in quadruplex formation, thereby indicating this oligonucleotide's ability to form G-quadruplex structure. Footprinting results indicate that in the presence of potassium ions, the segment harboring a putative G-quadruplex sequence does form G-quadruplex in vitro. The structure was found to be less prominent in lithium ions and nonexistent in the presence of magnesium ions. Bioinformatic prediction, followed by biophysical characterization and footprinting analysis, confirms the existence of an intramolecular quadruplex in the TGFβ 5′ UTR.

G-Quadruplex-Forming Sequence Inhibits the Translational Efficiency of the Renilla Luciferase Reporter Gene in HEK 293T and MCF-7 Cells. To assay the role of G-quadruplex-forming sequence in modulating the translational

dx.doi.org/10.1021/bi301365g | *Biochemistry* 2013, 52, 1528−1538

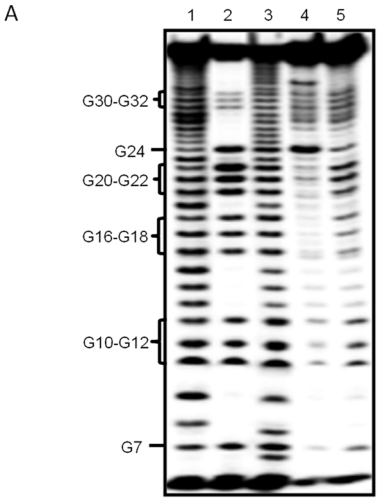

Figure 4. RNase T1 footprinting of 9-PG4−9 RNA. (A) Lanes 1 and 2 represent alkaline hydrolysis and RNase T1 ladders, respectively, while lanes 3−5 represent quadruplexes preformed in the presence of different ions. The concentrations of ions were 1 mM Mg^{2+} (lane 3), 150 mM K^{+} (lane 4), and 150 mM Li^{+} (lane 5). (B) Sequence of the 9-PG4−9 RNA used for footprinting studies. Guanine residues predicted to form the quadruplex structure are colored red.

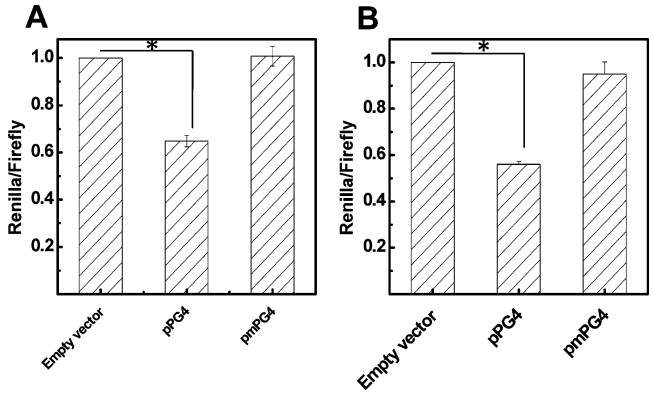

Figure 5. Inhibition of translation of the luciferase reporter gene in the presence of the RNA G-quadruplex motif alone. (A) HEK 293T and (B) MCF-7 cell lines were transfected with pPG4 and pmPG4 plasmid constructs, and after incubation for 48 h, the dual luciferase assay was performed with the cell lysate. Renilla luciferase activity was normalized to firefly luciferase activity. The experiments were performed in triplicate, and results are expressed as means ± the standard error. Asterisks indicate statistical significance (Student's *t* test) relative to empty vector-transfected cells ($*p < 0.01$).

efficiency of the reporter gene, we inserted the PG4 sequence into the NheI site upstream of the Renilla luciferase gene in the psiCHECK-2 vector. As a control, the mPG4 construct was made with mutations that disrupt G-quadruplex formation. These constructs were transfected into HEK 293T and MCF-7 cells. After incubation for 48 h, the luciferase assay was performed using the cell lysate. The HEK 293T cell line was chosen for its high tranfection efficiency, and the MCF-7 cell line was preferred because TGFβ2 is known to be overexpressed in breast cancer cells. Transfection of HEK 293T and MCF-7 cells with the pPG4 construct reduced the Renilla luciferase reporter gene activity normalized to firefly luciferase activity to 65% and 56%, respectively (Figure 5). Transfection with the pmPG4 construct restored the expression level of the Renilla luciferase gene to a level similar to that of the empty vector in both cell lines.

G-Quadruplex-Forming Sequence in the Context of the Entire TGFβ2 5′ UTR Augments the Translational Efficiency of the Renilla Luciferase Reporter Gene in HEK 293T and MCF-7 Cells. To determine the function of the G-quadruplex in the context of the entire 5′ UTR of TGFβ2 in cells, we assessed the gene expression of the Renilla luciferase enzyme at the mRNA and protein level. The entire 5′ UTR region of TGFβ2 was cloned into the NheI site upstream of the Renilla luciferase gene in the psiCHECK-2 vector. As a control, site mutations G314A, G320A, G324A, and G334A were introduced into the G-quadruplex-forming sequence in the 5′ UTR. In addition, construct pUTRΔPG4 with the entire 5′ UTR minus a 23-nucleotide G-quadruplex sequence was also synthesized. These vectors, namely, pwtUTR, pUTRΔPG4, and pmUTR, were transfected into the HEK 293T and MCF-7 cells, and cell lysates were used for the luciferase assay after incubation for 48 h. Interestingly, transfections of pwtUTR in comparison to pmUTR showed an increase in the level of Renilla luciferase expression. The presence of RNA G-quadruplex in the 5′ UTR of the reporter gene significantly increased Renilla/firefly activity to 172% and 198% in HEK 293T and MCF-7 cells, respectively (Figure 6). To further confirm the role of the G-quadruplex, we generated two additional mutant plasmids, pG313AUTR and pG313A,G321AUTR, harboring one and two point mutations, respectively, in the PG4 sequence in the 5′ UTR of TGFβ2. These mutant plasmids significantly increased Renilla/firefly activity to 117% and 128% in MCF-7 cells. Thus, this G-quadruplex-induced increase in the level of expression of the reporter gene confers a completely different role to the RNA G-quadruplex in the context of the entire 5′ UTR. It shows that the G-quadruplex in the context of the entire 5′ UTR of TGFβ2 acts as an enhancer of gene expression.

To assess the changes in the mRNA levels of the Renilla luciferase gene in the transfected cells with these constructs, we performed real-time PCR (RT-PCR). As shown in Figure 7, there was no significant difference in the relative level of Renilla luciferase mRNA in the transfected cells with different constructs. Thus, the possibility of G-quadruplex sequence and 5′ UTR as a whole affecting transcription of reporter gene was negated by quantitative RT-PCR results. RT-PCR showed a similar relative mRNA level of the Renilla luciferase gene in the cell line transfected with different plasmid constructs.

TmPyP4 Binds with PG4 RNA in Vitro. UV titration is a technique commonly used to understand the binding parameters of a nucleic acid with a ligand. Here, we studied the binding behavior of the ligand TmPyP4 with PG4 RNA. Figure S6 of the Supporting Information shows the changes in the intensity and wavelength of the absorption band of TmPyP4 with stepwise additions of PG4 RNA. The interaction of TmPyP4 with PG4 RNA induced 81% hypochromicity and a 19 nm red shift in the Soret band (421 nm) of TmPyP4. An isosbestic point was seen at 437 nm. This titration study clearly shows that TmPyP4 binds with the PG4 RNA G-quadruplex.

TmPyP4 Treatment Did Not Cause Any Significant Changes in the Reporter Gene Expression Profile of Transfected MCF-7 Cells. Basu and co-workers[67] have shown that cationic porphyrin TmPyP4 binds and unfolds the RNA G-quadruplex in the 5′ UTR of MT3-MMP, thereby relieving the inhibitory effect of the MT3-MMP RNA G-quadruplex. To assess the effect of TmPyP4 on the TGFβ2 RNA G-quadruplex, MCF-7 cells were transfected with plasmids (pwtUTR, pmUTR,

dx.doi.org/10.1021/bi301365g | *Biochemistry* 2013, 52, 1528−1538

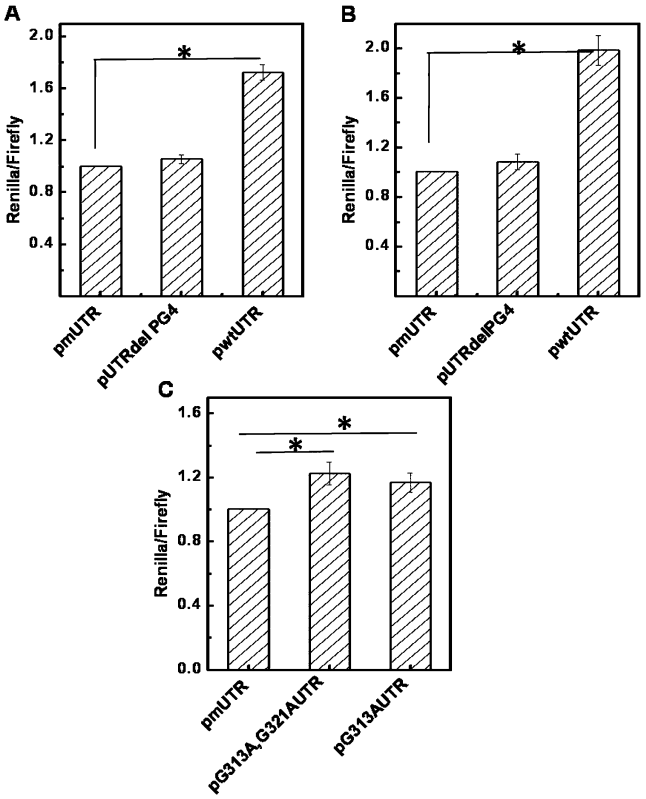

Figure 6. Augmentation of translation of the luciferase reporter gene by the G-quadruplex motif in the context of the entire 5′ UTR of TGFβ2. (A) HEK 293T and (B) MCF-7 cell lines were transfected with pwtUTR, pUTRΔPG4, and pmUTR plasmid constructs, and after incubation for 48 h, the dual luciferase assay was performed with the cell lysate. (C) MCF-7 cell lines were transfected with pmUTR, pG313AUTR, and pG313A,G321AUTR plasmids, and the dual luciferase assay was performed with the cell lysate. Renilla luciferase activity was normalized to firefly luciferase activity. The experiments were performed in triplicate, and results are expressed as means ± the standard error. Asterisks indicate statistical significance (Student's *t* test) relative to pmUTR-transfected cells ($*p < 0.05$).

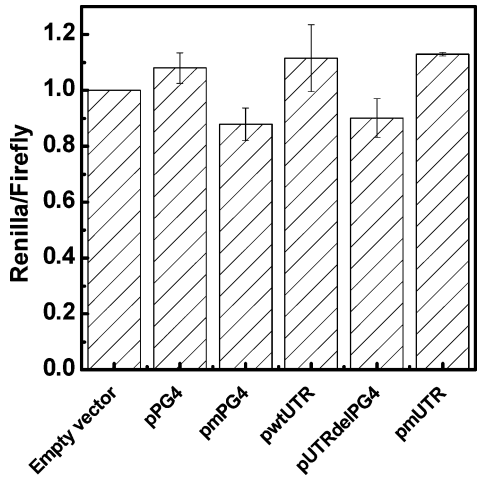

Figure 7. Quantification of the mRNA level of the luciferase reporter gene employing RT-PCR. MCF-7 cells were transfected with various plasmid constructs, and RNA was isolated after incubation for 48 h. cDNA was prepared, and the mRNA level of the reporter gene was estimated by RT-PCR using Renilla and firefly luciferase gene specific primers. The Renilla/firefly transcript level ratio was calculated and normalized using the Pfaffl method. RT-PCR showed a similar mRNA level of the Renilla luciferase gene in the cell line transfected with different plasmid constructs. These quantitative RT-PCR results negate the possibility of G-quadruplex sequence and 5′ UTR as a whole to affect transcription of the reporter gene. The experiments were performed in triplicate, and results are expressed as means ± the standard error.

and pUTRΔPG4) and thereafter treated with varying concentrations of this ligand. Surprisingly, a dual luciferase assay with these cell lysates did not show any significant changes in the reporter gene expression. This study suggests that TmPyP4 does not interfere with the RNA G-quadruplex in the 5′ UTR of TGFβ2 (Figure S7 of the Supporting Information).

DISCUSSION

Selective targeting of TGFβ2 has been shown to prevent progressive renal disease.[59,60] Hau et al. used an antisense oligonucleotide to specifically target TGFβ2 and showed that TGFβ2 inhibition increased the survival time of patients suffering from recurrent or refractory malignant gliomas.[61,62] Also, resveratrol was reported to target TGFβ2 in cancer cells.[48,63] This shows drugs designed against this molecule may be therapeutically efficient for the treatment of invasive tumors. Along this line, the RNA G-quadruplex may act as a potential target for the design of a therapeutic drug for cancer patients.

The RNA G-quadruplex has been to shown to exist in the 5′ UTR of various genes and thereby modulate their gene expression.[7−17] TGFβ2 mRNA also harbors a 23-nucleotide G-quadruplex-forming sequence in its 5′ UTR. Biophysical characterization of this putative G-quadruplex sequence demonstrates its ability to form a stable intramolecular G-quadruplex in vitro. Additionally, the CD signature of PG4 RNA obeys the parallel conformation of the RNA G-quadruplex. The plausible reason for this monomorphic nature is the inability of riboguanines involved in quadruplex formation to adopt the syn conformation, a prerequisite for antiparallel G-quadruplex formation.[64] Also, melting experiments displayed a T_m of 64 ± 1 °C (in the presence of 25 mM KCl), an indication of its ability to form a highly stable structure. We found the T_m of TGFβ2 PG4 to be comparable with that of the RNA G-quadruplex sequence present in the 5′ UTR of other genes reported in the literature. The T_m of Zic-1 PG4 in 25 mM KCl is 79 °C,[8] whereas the RNA G-quadruplex sequences in the 5′ UTR of ADAM-10 and MT3-MMP have T_m values of 60 °C and 72 °C, respectively, in 1 mM KCl.[12,16]

We showed that the 23-nucleotide PG4 sequence retains its ability to form G-quadruplex in the presence of a neighboring nucleotide sequence. Sugimoto and co-workers have previously shown in biophysical studies that in the 5′ UTR of some protooncogenes, the GC-rich RNA sequences form stable A-form duplexes as the predominant structure under various environmental conditions.[65] Bioinformatic prediction of only a short stretch of RNA does not take into consideration the contribution of flanking nucleotide sequence in stabilizing this secondary structure. Hence, to understand more closely the formation and stabilization of the G-quadruplex in the presence of a flanking nucleotide sequence, we sought to perform spectroscopic and gel-based footprinting analysis of PG4 with flanks on either end. UV and CD spectroscopy supported the quadruplex forming ability of PG4 with nine-nucleotide flanks on either end. This addition of nine-nucleotide flanks on either end increased the T_m of PG4 RNA by 5 °C, demonstrating greater stabilization of G-quadruplex structure in presence of flanking sequence. Thus, unlike the destabilizing effect of flanking

dx.doi.org/10.1021/bi301365g | *Biochemistry* 2013, 52, 1528−1538

sequence on DNA G-quadruplex,[58] the neighboring nucleotide sequence of the G-quadruplex enhances the stability of the RNA G-quadruplex. Footprinting analysis of these oligonucleotides further showed RNase T1-induced cleavage protection at guanine residues predicted to be involved in G-quadruplex formation. The cleavage protection was found to be more prominent in potassium buffer than in lithium buffer, further supporting the evidence of G-quadruplex formation. In a nutshell, we showed that unlike DNA quadruplex sequence, RNA PG4 sequence in the 5′ UTR of TGFβ2 maintains its ability to form a G-quadruplex even in the presence of a long neighboring sequence.

After the structural characterization of the RNA G-quadruplex, we performed a dual luciferase assay for its functional validation. As in previous studies,[8,12,16] here we used the dual luciferase system to decipher the functional implication of the RNA G-quadruplex in the 5′ UTR of TGFβ2. PG4 alone inhibited the expression of the reporter Renilla luciferase enzyme in accordance with the previously published results.[8,12] However, contrary to established repressive roles of the G-quadruplex in the 5′ UTR,[7,10,12,13,15,16] the presence of PG4 in the 5′ UTR increased the level of expression of the reporter gene. Thus, these observations confer an enhancer role to the RNA G-quadruplex in the 5′ UTR in regulating gene expression of TGFβ2. RT-PCR results indicate that G-quadruplex does not affect gene expression at the transcriptional level, validating the regulatory role of PG4 in gene expression exclusively at the translational level. In other words, this positive cis-regulatory function of the G-quadruplex in the 5′ UTR acts at the level of translation, augmenting gene expression.

Although the PG4 sequence per se showed its potential to form an intramolecular G-quadruplex and inhibit translation in cells, it augments gene expression in the context of the entire 5′ UTR. The mechanism for the augmentation is not known, but speculations can be made. This PG4 sequence behavior may be attributed to the location of the G-quadruplex sequence in the 5′ UTR of TGFβ2. Unlike the 5′ UTR of MT3-MMP, BCl-2, and ADAM-10,[12,13,16] the PG4 sequence lies far from the 5′ end of the UTR as well as from the translation start site of TGFβ2 mRNA. At this position, the G-quadruplex may recruit some interacting factors, thereby increasing the translational efficiency of the ribosome. Balasubramanian and co-workers have shown that the position of the PG4 sequence in the 5′ UTR of NRAS mRNA acts as a determining factor for its role in translational regulation.[66]

Furthermore, to assess the binding behavior of PG4 RNA with a known G-quadruplex ligand TmPyP4, we performed UV−vis absorption titration experiments. A large red shift of 19 nm and a hypochromicity of 81% clearly indicated the binding of TmPyP4 with PG4 RNA.[54] However, when we treated the transfected cells with varying concentrations of this ligand, we obtained unexpected results. Although in vitro studies show binding of TmPyP4 to PG4 RNA, there was no significant difference in the reporter gene expression profile of transfected cells upon treatment with this ligand. Unlike its destabilizing effect on the RNA G-quadruplex in MT3-MMP,[67] TmPyP4 did not interfere with RNA G-quadruplex function in the 5′ UTR of TGFβ2, suggesting its low selectivity for the TGFβ2 RNA G-quadruplex under in cellulo conditions.

The presence of the G-quadruplex in the 5′ UTR is generally associated with the inhibition of cap-dependent translation. However, Morris et al. reported the essentiality of the 5′ UTR-located switchable G-quadruplex in IRES-mediated cap-independent translation of VEGF.[14] They proposed that specific combinations of G-tracts can be used to fine-tune the translational initiation of VEGF.

In this study, G-quadruplex-forming sequence at position 313 from the 5′ end of TGFβ2 mRNA involves four GGG tracts with intermittent variable loop lengths. Unlike VEGF, this sequence is unable to form conformationally flexible G-quadruplex structures to regulate translational initiation. Moreover, the VEGF G-quadruplex study is based on the usage of a sequence involved in IRES-mediated cap-independent translation. No report showing cap-independent translation in TGFβ2 is available in the literature. Furthermore, unknown factors like molecular partners, cellular milieu, and spatiotemporal requirements may promote the establishment of the lesser known activating role of the 5′ UTR G-quadruplex in TGFβ2.

Hence, this report describes a novel mechanism of gene regulation at the translational level. The G-quadruplex in the 5′ UTR is required for the enhanced expression of TGFβ2. Its conformational disruption leads to the repression of gene expression. Although the 5′ UTR region of TGFβ2 mRNA is unusually long (1368 nucleotides) and GC-rich, any conclusive remark about its mode of translation cannot be drawn from this study. To conclude, without the involvement of IRES, the G-quadruplex in the 5′ UTR of TGFβ2 may set a prototypic example of a positive regulator of cap-dependent translation. Like the strategies used to directly target TGFβ2 expression in invasive tumors,[48,62,63] selectively targeting this RNA G-quadruplex in the 5′ UTR of TGFβ2 with small molecules may provide for better therapeutics in the future. To this end, a quest for the development of selective RNA G-quadruplex ligands that will specifically interfere with these structures in cells is essential.

■ ASSOCIATED CONTENT

Supporting Information

Primers used for cloning and RT-PCR (Tables S1 and S2) and CD melting profile of PG4 RNA, mPG4 RNA, 9-PG4−9RNA, and m9-PG4−9 RNA (Figure S1). This material is available free of charge via the Internet at http://pubs.acs.org.

■ AUTHOR INFORMATION

Corresponding Author

*Proteomics and Structural Biology Unit, Institute of Genomics and Integrative Biology, CSIR, Mall Road, Delhi, India. Telephone: +91 11 27666156. Fax: +91 11 27667437. E-mail: souvik@igib.res.in.

Funding

This work was financially supported by Project BSC0123 from the Council of Scientific and Industrial Research (CSIR), Government of India, and by the Swarnajayanti project to S.M. from the Department of Science and Technology (DST), Government of India.

Notes

The authors declare no competing financial interest.

■ ACKNOWLEDGMENTS

We thank Professor Soumitra Basu (Kent State University, Kent, OH) for providing suggestions for footprinting experiments.

■ ABBREVIATIONS

TGFβ2, transforming growth factor β2; UTR, untranslated region; CD, circular dichroism; TDS, thermal difference

spectrum; T_m, melting temperature; PG4, putative G-quadruplex; FP, forward primer; RP, reverse primer.

REFERENCES

(1) Smith, F. W., and Feigon, J. (1992) Quadruplex structure of Oxytricha telomeric DNA oligonucleotides. *Nature 356*, 164−168.

(2) Wieland, M., and Hartig, J. S. (2009) RNA quadruplex-based modulation of gene expression. *Nat. Protoc. 4*, 1632−1640.

(3) Gellert, M., Lipsett, M. N., and Davies, D. R. (1962) Helix formation by guanylic acid. *Proc. Natl. Acad. Sci. U.S.A. 48*, 2013−2018.

(4) Liu, H., Kanagawa, M., Matsugami, S., Tanaka, Y., Katahira, M., and Uesugi, S. (2000) NMR study of a novel RNA quadruplex structure. *Nucleic Acids Symp. Ser. 44*, 65−66.

(5) Collie, G. W., Haider, S. M., Neidle, S., and Parkinson, G. N. (2010) A crystallographic and modelling study of a human telomeric RNA (TERRA) quadruplex. *Nucleic Acids Res. 38*, 5569−5580.

(6) Bonnal, S., Schaeffer, C., Creancier, L., Clamens, S., Moine, H., Prats, A. C., and Vagner, S. (2003) A single internal ribosome entry site containing a G quartet RNA structure drives fibroblast growth factor 2 gene expression at four alternative translation initiation codons. *J. Biol. Chem. 278*, 39330−39336.

(7) Kumari, S., Bugaut, A., Huppert, J. L., and Balasubramanian, S. (2007) An RNA G-quadruplex in the 5′ UTR of the NRAS proto-oncogene modulates translation. *Nat. Chem. Biol. 3*, 218−221.

(8) Arora, A., Dutkiewicz, M., Scaria, V., Hariharan, M., Maiti, S., and Kurreck, J. (2008) Inhibition of translation in living eukaryotic cells by an RNA G-quadruplex motif. *RNA 14*, 1290−1296.

(9) Balkwill, G. D., Derecka, K., Garner, T. P., Hodgman, C., Flint, A. P., and Searle, M. S. (2009) Repression of translation of human estrogen receptor α by G-quadruplex formation. *Biochemistry 48*, 11487−11495.

(10) Derecka, K., Balkwill, G. D., Garner, T. P., Hodgman, C., Flint, A. P., and Searle, M. S. (2010) Occurrence of a quadruplex motif in a unique insert within exon C of the bovine estrogen receptor α gene (ESR1). *Biochemistry 49*, 7625−7633.

(11) Halder, K., Wieland, M., and Hartig, J. S. (2009) Predictable suppression of gene expression by 5′-UTR-based RNA quadruplexes. *Nucleic Acids Res. 37*, 6811−6817.

(12) Morris, M. J., and Basu, S. (2009) An unusually stable G-quadruplex within the 5′-UTR of the MT3 matrix metalloproteinase mRNA represses translation in eukaryotic cells. *Biochemistry 48*, 5313−5319.

(13) Shahid, R., Bugaut, A., and Balasubramanian, S. (2010) The BCL-2 5′ untranslated region contains an RNA G-quadruplex-forming motif that modulates protein expression. *Biochemistry 49*, 8300−8306.

(14) Morris, M. J., Negishi, Y., Pazsint, C., Schonhoft, J. D., and Basu, S. (2010) An RNA G-quadruplex is essential for cap-independent translation initiation in human VEGF IRES. *J. Am. Chem. Soc. 132*, 17831−17839.

(15) Gomez, D., Guédin, A., Mergny, J. L., Salles, B., Riou, J. F., Teulade-Fichou, M. P., and Calsou, P. (2010) A G-quadruplex structure within the 5′-UTR of TRF2 mRNA represses translation in human cells. *Nucleic Acids Res. 38*, 7187−7198.

(16) Lammich, S., Kamp, F., Wagner, J., Nuscher, B., Zilow, S., Ludwig, A. K., Willem, M., and Haass, C. (2011) Translational repression of the disintegrin and metalloprotease ADAM10 by a stable G-quadruplex secondary structure in its 5′-untranslated region. *J. Biol. Chem. 286*, 45063−45072.

(17) Arora, A., and Suess, B. (2011) An RNA G-quadruplex in the 3′UTR of the proto-oncogene PIM1 represses translation. *RNA Biol. 8*, 802−805.

(18) Christiansen, J., Kofod, M., and Nielsen, F. C. (1994) A guanosine quadruplex and two stable hairpins flank a major cleavage site in insulin-like growth factor II mRNA. *Nucleic Acids Res. 22*, 5709−5716.

(19) Decorsière, A., Cayrel, A., Vagner, S., and Millevoi, S. (2011) Essential role for the interaction between hnRNP H/F and a G quadruplex in maintaining p53 pre-mRNA 3′-end processing and function during DNA damage. *Genes Dev. 25*, 220−225.

(20) Wanrooij, P. H., Uhler, J. P., Simonsson, T., Falkenberg, M., and Gustafsson, C. M. (2010) G-quadruplex structures in RNA stimulate mitochondrial transcription termination and primer formation. *Proc. Natl. Acad. Sci. U.S.A. 107*, 16072−16077.

(21) Min, H., Chan, R. C., and Black, D. L. (1995) The generally expressed hnRNP F is involved in a neural-specific pre-mRNA splicing event. *Genes Dev. 9*, 2659−2671.

(22) Gomez, D., Lemarteleur, T., Lacroix, L., Mailliet, P., Mergny, J. L., and Riou, J. F. (2004) Telomerase downregulation induced by the G-quadruplex ligand 12459 in A549 cells is mediated by hTERT RNA alternative splicing. *Nucleic Acids Res. 32*, 371−379.

(23) Didiot, M. C., Tian, Z., Schaeffer, C., Subramanian, M., Mandel, J. L., and Moine, H. (2008) The G-quartet containing FMRP binding site in FMR1 mRNA is a potent exonic splicing enhancer. *Nucleic Acids Res. 36*, 4902−4912.

(24) Marcel, V., Tran, P. L. T., Sagne, C., Martel-Planche, G., Vaslin, L., Teulade-Fichou, M. P., Hall, J., Mergny, J. L., Hainaut, P., and Van Dyck, E. (2011) G-quadruplex structures in TP53 intron 3: Role in alternative splicing and in production of p53 mRNA isoforms. *Carcinogenesis 32*, 271−278.

(25) Subramanian, M., Rage, F., Tabet, R., Flatter, E., Mandel, J. L., and Moine, H. (2011) G-quadruplex RNA structure as a signal for neurite mRNA targeting. *EMBO Rep. 12*, 697−704.

(26) Darnell, J. C., Jensen, K. B., Jin, P., Brown, V., Warren, S. T., and Darnell, R. B. (2001) Fragile X mental retardation protein targets G quartet mRNAs important for neuronal function. *Cell 107*, 489−499.

(27) Schaeffer, C., Bardoni, B., Mandel, J. L., Ehresmann, B., Ehresmann, C., and Moine, H. (2001) The fragile X mental retardation protein binds specifically to its mRNA via a purine quartet motif. *EMBO J. 20*, 4803−4813.

(28) Melko, M., and Bardoni, B. (2010) The role of G-quadruplexes in RNA metabolism: Involvement of FMRP and FMR2P. *Biochimie 92*, 919−926.

(29) Xu, Y., Suzuki, Y., Ito, K., and Komiyama, M. (2010) Telomeric repeat-containing RNA structure in living cells. *Proc. Natl. Acad. Sci. US.A. 107*, 14579−14584.

(30) López de Silanes, I., Stagno d'Alcontres, M., and Blasco, M. A. (2010) TERRA transcripts are bound by a complex array of RNA-binding proteins. *Nat. Commun. 1*, 33.

(31) Deng, Z., Norseen, J., Wiedmer, A., Riethman, H., and Lieberman, P. M. (2009) TERRA RNA binding to TRF2 facilitates heterochromatin formation and ORC recruitment at telomeres. *Mol. Cell 35*, 403−415.

(32) Patel, D. J., Phan, A. T., and Kuryavyi, V. (2007) Human telomere, oncogenic promoter and 5′-UTR G-quadruplexes: Diverse higher order DNA and RNA targets for cancer therapeutics. *Nucleic Acids Res. 35*, 7429−7455.

(33) Agarwal, T., Jayaraj, G., Pandey, S. P., Agarwala, P., and Maiti, S. (2012) RNA G-quadruplexes: G-quadruplexes with "U" turns. *Curr. Pharm. Des. 18*, 2102−2111.

(34) Huppert, J. L., Bugaut, A., Kumari, S., and Balasubramanian, S. (2008) G-quadruplexes: The beginning and end of UTRs. *Nucleic Acids Res. 36*, 6260−6268.

(35) Massague, J. (2008) TGFβ in Cancer. *Cell 134*, 215−230.

(36) Thompson, H. G., Mih, J. D., Krasieva, T. B., Tromberg, B. J., and George, S. C. (2006) Epithelial-derived TGF-β2 modulates basal and wound-healing subepithelial matrix homeostasis. *Am. J. Physiol. 291*, L1277−L1285.

(37) Austin, A. F., Compton, L. A., Love, J. D., Brown, C. B., and Barnett, J. V. (2008) Primary and Immortalized Mouse Epicardial Cells Undergo Differentiation in Response to TGFβ. *Dev. Dyn. 237*, 366−376.

(38) Sanford, L. P., Ormsby, I., Gittenberger-de Groot, A. C., Sariola, H., Friedman, R., Boivin, G. P., Cardell, E. L., and Doetschman, T. (1997) TGFβ2 knockout mice have multiple developmental defects that are nonoverlapping with other TGFβ2 knockout phenotypes. *Development 124*, 2659−2670.

(39) Bartram, U., Molin, D. G., Wisse, L. J., Mohamad, A., Sanford, L. P., Doetschman, T., Speer, C. P., Poelmann, R. E., and Gittenberger-de Groot, A. C. (2001) Double-Outlet Right Ventricle and Overriding Tricuspid Valve Reflect Disturbances of Looping, Myocardialization, Endocardial Cushion Differentiation, and Apoptosis in TGF-β2-Knockout Mice. *Circulation 103*, 2745−2752.

(40) Saika, S. (2006) TGFβ pathobiology in the eye. *Lab. Invest. 86*, 106−115.
(41) Constam, D. B., Philipp, J., Malipiero, U. V., Dijke, P., Schachner, M., and Fontana, A. (1992) Differential expression of transforming growth factor-β1, -β2, and -β3 by glioblastoma cells, astrocytes, and microglia. *J. Immunol. 148*, 1404−1410.
(42) Wick, W., Naumann, U., and Weller, M. (2006) Transforming growth factor-β: A molecular target for the future therapy of glioblastoma. *Curr. Pharm. Des. 12*, 341−349.
(43) Penuelas, S., Anido, J., Prieto-Sanchez, R. M., Folch, G., Barba, I., Cuartas, I., García-Dorado, D., Poca, M. A., Sahuquillo, J., Baselga, J., and Seoane, J. (2009) TGF-β increases glioma-initiating cell self-renewal through the induction of LIF in human glioblastoma. *Cancer Cell 15*, 315−327.
(44) Frey, R. S., and Mulder, K. M. (1997) TGFβ regulation of mitogen-activated protein kinases in human breast cancer cells. *Cancer Lett. 117*, 41−50.
(45) Buck, M. B., and Knabbe, C. (2006) TGF-β Signaling in Breast Cancer. *Ann. N.Y. Acad. Sci. 1089*, 119−126.
(46) Von Bernstorff, W., Voss, M., Freichel, S., Schmid, A., Vogel, I., Jöhnk, C., Henne-Bruns, D., Kremer, B., and Kalthoff, H. (2001) Systemic and local immunosuppression in pancreatic cancer patients. *Clin. Cancer Res. 7*, 925s−932s.
(47) Jonson, T., Albrechtsson, E., Axelson, J., Heidenblad, M., Gorunova, L., Johansson, B., and Höglund, M. (2001) Altered expression of TGFB receptors and mitogenic effects of TGFB in pancreatic carcinomas. *Int. J. Oncol. 19*, 71−81.
(48) Kim, K. H., Back, J. H., Zhu, Y., Arbesman, J., Athar, M., Kopelovich, L., Kim, A. L., and Bickers, D. R. (2011) Resveratrol targets transforming growth factor-β2 signaling to block UV-induced tumor progression. *J. Invest. Dermatol. 131*, 195−202.
(49) Lu, T., Burdelya, L. G., Swiatkowski, S. M., Boiko, A. D., Howe, P. H., Stark, G. R., and Gudkov, A. V. (2004) Secreted transforming growth factor β2 activates NF-κB, blocks apoptosis, and is essential for the survival of some tumor cells. *Proc. Natl. Acad. Sci. U.S.A. 101*, 7112−7117.
(50) Kim, K. H., Back, J. H., Zhu, Y., Arbesman, J., Athar, M., Kopelovich, L., Kim, A. L., and Bickers, D. R. (2001) Resveratrol targets transforming growth factor-β2 signaling to block UV-induced tumor progression. *J. Invest. Dermatol. 131*, 195−202.
(51) Beisner, J., Buck, M. B., Fritz, P., Dippon, J., Schwab, M., Brauch, H., Zugmaier, G., Pfizenmaier, K., and Knabbe, C. (2006) A novel functional polymorphism in the transforming growth factor-β2 gene promoter and tumor progression in breast cancer. *Cancer Res. 66*, 7554−7561.
(52) Wang, B., Koh, P., Winbanks, C., Coughlan, M. T., McClelland, A., Watson, A., Jandeleit-Dahm, K., Burns, W. C., Thomas, M. C., Cooper, M. E., and Kantharidis, P. (2011) miR-200a prevents renal fibrogenesis through repression of TGF-β2 expression. *Diabetes 60*, 280−287.
(53) Scaria, V., Hariharan, M., Arora, A., and Maiti, S. (2006) Quadfinder: Server for identification and analysis of quadruplex-forming motifs in nucleotide sequences. *Nucleic Acids Res. 34*, W683−W685.
(54) Arora, A., and Maiti, S. (2009) Differential biophysical behavior of human telomeric RNA and DNA quadruplex. *J. Phys. Chem. B 113*, 10515−10520.
(55) Pfaffl, M. W. (2001) A new mathematical model for relative quantification in real-time RT-PCR. *Nucleic Acids Res. 29*, e45.
(56) Mergny, J. L., Phan, A. T., and Lacroix, L. (1998) Following G-quartet formation by UV-spectroscopy. *FEBS Lett. 435*, 74−78.
(57) Mergny, J. L., Li, J., Lacroix, L., Amrane, S., and Chaires, J. B. (2005) Thermal difference spectra: A specific signature for nucleic acid structures. *Nucleic Acids Res. 33*, e138.
(58) Arora, A., Nair, D. R., and Maiti, S. (2009) Effect of flanking bases on quadruplex stability and Watson-Crick duplex competition. *FEBS J. 276*, 3628−3640.
(59) Ledbetter, S., Kurtzberg, L., Doyle, S., and Pratt, B. M. (2000) Renal fibrosis in mice treated with human recombinant transforming growth factor-β2. *Kidney Int. 58*, 2367−2376.
(60) Hill, C., Flyvbjerg, A., Rasch, R., Bak, M., and Logan, A. (2001) Transforming growth factor-β2 antibody attenuates fibrosis in the experimental diabetic rat kidney. *J. Endocrinol. 170*, 647−651.
(61) Schlingensiepen, K. H., Schlingensiepen, R., Steinbrecher, A., Hau, P., Bogdahn, U., Fischer-Blass, B., and Jachimczak, P. (2006) Targeted tumor therapy with the TGF-β2 antisense compound AP 12009. *Cytokine Growth Factor Rev. 17*, 129−139.
(62) Hau, P., Jachimczak, P., and Bogdahn, U. (2009) Treatment of malignant gliomas with TGF-β2 antisense oligonucleotides. *Expert Rev. Anticancer Ther. 9*, 1663−1674.
(63) Serrero, G., and Lu, R. (2001) Effect of resveratrol on the expression of autocrine growth modulators in human breast cancer cells. *Antioxid. Redox Signaling 3*, 969−979.
(64) Tang, C. F., and Shafer, R. H. (2006) Engineering the quadruplex fold: Nucleoside conformation determines both folding topology and molecularity in guanine quadruplexes. *J. Am. Chem. Soc. 128*, 5966−5973.
(65) Saxena, S., Miyoshi, D., and Sugimoto, N. (2010) Sole and stable RNA duplexes of G-rich sequences located in the 5′-untranslated region of protooncogenes. *Biochemistry 49*, 7190−7201.
(66) Kumari, S., Bugaut, A., and Balasubramanian, S. (2008) Position and stability are determining factors for translation repression by an RNA G-quadruplex-forming sequence within the 5′ UTR of the NRAS proto-oncogene. *Biochemistry 47*, 12664−12669.
(67) Morris, M. J., Wingate, K. L., Silwal, J., Leeper, T. C., and Basu, S. (2012) The porphyrin TmPyP4 unfolds the extremely stable G-quadruplex in MT3-MMP mRNA and alleviates its repressive effect to enhance translation in eukaryotic cells. *Nucleic Acids Res. 40*, 4137−4145.